Structural Eng. / Earthquake Eng. Vol. 5. No. 1, 81s-87s. April 1988
Japan Society of Civil Engineers (Proc. of JSCE No. 392/I-9)

ULTIMATE STRENGTH DESIGN PROVISIONS FOR FIXED-END STEEL ARCHES WITH VARIABLE CROSS-SECTIONS

By Tetsuya YABUKI and Shigeru KURANISHI***

First of all, size and change location of cover plates which compose variable box cross sections adopted in fixed-end steel arch ribs are examined using their core-moments analyzed by a first-order-elastic analysis. Then, strain behavior at ultimate states of the arches with several patterns of the variable cross-sections are discussed using an ultimate strength analysis. Relationships between the ultimate strengths of the arches with variable cross-sections and those of arches with uniform cross-sections are also investigated. Based on the results a practical estimate on their relationships is carried out. Finally presented are design provisions which are able to take into account the effects of the variable cross-section on the ultimate strength.

Keywords: *arch bridge, steel structure, compression member, structural stability, limit state design*

1. INTRODUCTION

Considerable research has carried out on fixed-end steel arches with uniform cross-sections to determine their ultimate strengths[1),2)]. The behavior on the over-all, in-plane ultimate strength of arch ribs is characterized by failing by instability under combined axial compression and bending moment. For the fixed arches with uniform cross-sections, the design criterion formulated by the combined member forces is now available to determine its ultimate strength[3)]. However, for fixed arches with variable cross-sections, no rational procedure based on this instability concept has been developed.

In designing fixed-end steel arch ribs based on linear stress concept, it is advantageous to use reduced cross sections over the rib except nearby its springings. In this study, first, it is performed to examine whether this advantage is expected until to the ultimate states of the fixed-end steel arches with variable cross sections, using an ultimate strength analysis developed in Refs. 2) and 3). Usually, depths of plate girders are restricted by critical width-to-thickness ratios for web plate bucklings, and provided as deeply as possible within the restriction because of its efficiency for bending capacity. Thus, the variable cross sections are generally provided by reduced thickness of flange or cover plates and the same manner is adopted in this study. To examine local strain behavior at change-locations of the cover plate sizes, typical three patterns of the variable-sectioning manners are discussed:

i) Pattern A: $\alpha_1=\alpha_2$ at $(\beta_2+2\beta_1)L$, $\alpha_2\leqq 1$
ii) Pattern B: $\alpha_1=(1+\alpha_2)/2$ at $\beta_1 L$, $\alpha_2\leqq 1$
iii) Pattern C: $\alpha_1=1$ at $\beta_1 L$, $\alpha_2\leqq 1$

in which α_1 and α_2 are reduced thickness factors of the cover plates, and β_1 and β_2 their change location

* Member of JSCE, Dr. Eng., Professor, Department of Civil Engineering, University of Ryukyu (Okinawa).
** Member of JSCE, Dr. Eng., Professor, Department of Civil Engineering, Tohoku University (Sendai).

factors, as shown in Fig. 1. A reference cross section is proportioned along the rib from its springing to $\beta_0 L$. The patterns selected are generally within those found in fixed-end steel arch bridges. The fixed-end arch ribs selected for the study have the same as those adopted in Refs. 2) and 3) in all respects except their variable cross-sectioning.

Secondary, the in-plane, over-all, ultimate strengths of fixed arches with variable cross-sections under vertical loadings are discussed in comparison with those of fixed arches with uniform cross-sections ($\alpha_1=\alpha_2=1$)[2),3)]. Then, finally, a factor which is able to estimate the reduction in the strength of the fixed arch that results from partially reduced cross-sectioning is formulated. Thus, using this reduced strength factor, it is possible to utilize directly the available design formula for the fixed arches with uniform cross-sections.

2. EFFECTS OF VARIABLE SECTIONING

It is usually economical to reduce the size of the cover plates in the region of low moment in fixed arches. While, no specific rules can be made to help designers to determine when it is desirable to change the cover plate size. If only one change in the cover plate size is desired, a certain simple manner is possibly available. For simplicity in practical design of arches it is convenient to use so-called core-moment which makes it possible to evaluate combined axial force and bending moment. Fig. 2 shows a typical maximum core-moment diagram calculated by a first-order-elastic analysis, where the maximum moment, $M_{c,\max}$, is nondimensionalized by its value at the springing, $M^{f}_{c,\max}$. In the figure, an additional concentrated load, Q_L, is taken into account as a line load defined by the Japanese Highway Bridge Specification[4)], and a loading case which is a standard load intensity ratio of dead load to live plus dead loads for practical steel arch bridge ($r=0.75$) is adopted. The $M_{c,\max}$ is decided as the maximum value of the core-moments which are calculated for change of placed locations of the line load, Q_L, and distributed live load, $(1-r)q$, applied to the arch under the dead load, rq, as shown in the inset of Fig. 2. The highest value of $M_{c,\max}$ is computed at the springing and the reduced thickness can be used in the region of low moment, l_L, shown in the figure. Namely, the reference cross section is proportioned in the region of high moment, l_H.

By the preliminary study on linear stress conditions in the range of practical structural parameters for fixed-end steel arch bridges, it is observed that the regions of high moments, l_H, are within one-tenth of the spans and ratios of the low moments to the high moments are 0.65 approximately. Thus, the location factor of the reference cover plate thickness, β_0, as shown in Fig. 1 could be recommended to be equal to 0.1 and it is selected in the study. Moreover, it is also observed that the highest core-moment is given when the live load is roughly placed over one-half of the span. Thus, in what follows, the ultimate strengths are investigated under the loading manner as shown in Fig. 1 and the manner is same as adopted in Ref. 3).

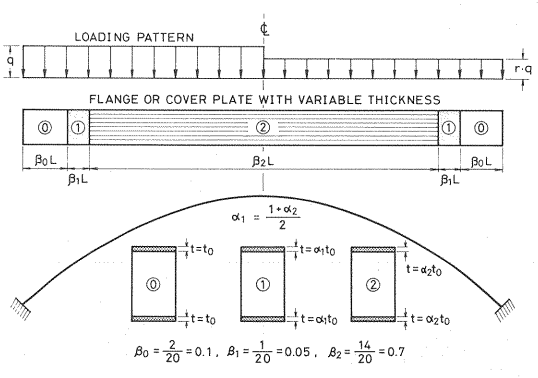

Fig. 1 Schematic Diagram of Variable Cross-sectioning.

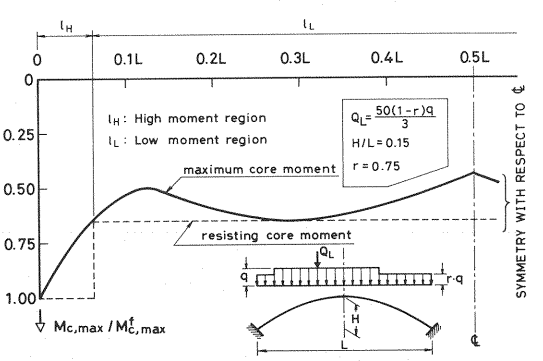

Fig. 2 Diagram of Maximum Core-Moments.

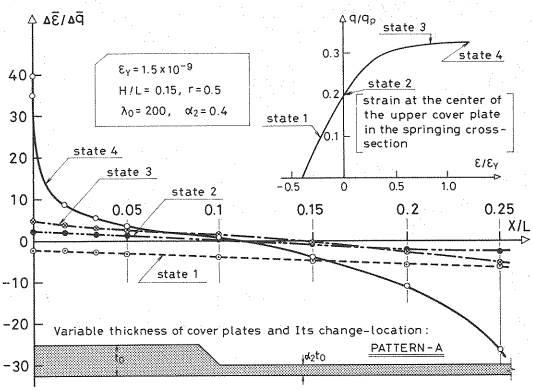

Fig. 3 Incremental Strain Mode at each Loading Step (for variable cross-section of PATTERN-A).

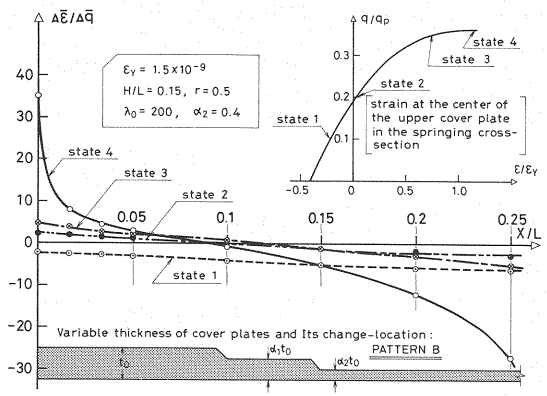

Fig. 4 Incremental Strain Mode at each Loading Step (for variable cross-section of PATTERN-B).

Figs. 3, 4 and 5 show typical nondimensional forms of incremental strains at the middle of the upper cover plate cross section along a fixed arch span from the springing to the one-quarter of the span for a slenderness ratio $\lambda_0=200$, a rise-to-span ratio $H/L=0.15$, an yield strain $\varepsilon_Y=1.5\times10^{-9}$, a load intensity ratio $r=0.5$ and a reduced thickness factor $\alpha_2=0.4$—incremental strain mode—from low level loading state to the ultimate state. Fig. 3 is a case of the variable cross-sectional Pattern A, and Figs. 4 and 5 the Patterns B and C, respectively. Where, the slenderness ratio λ_0 is the ratio of the curvilinear length of the arch axis to the radius of gyration of the cross section at the springing and is the same for an arch with variable cross-section or uniform cross-section. In the figures, the mode is given by dividing the nondimensional incremental strain ($\Delta\bar{\varepsilon}=\Delta\varepsilon/\varepsilon_Y$) by the dimensionless incremental load intensity ($\Delta\bar{q}=\Delta q/q_p$, q_p=the intensity of the discrete, uniform load over the entire span that produces full plastic axial thrust at the springing of the arch[3]). From Figs. 3, 4 and 5 it can be seen that the each incremental strain mode of the Patterns A, B and C is smoothly varied over the span length up to the ultimate state. Thus, simultaneously considering the linear stress-approach mentioned earlier, the Pattern A is seemed to be suitable for the variable cross-sectioning manner. However, considering so-called fatigue resistance problems or stress concentration problems or both for large-sized cover-plated beam members, the Pattern B might be more adequate for fixed-end steel arch bridges. Hereafter in the study, therefore, the ultimate strength of the fixed-end arch ribs with the variable cross section of Pattern B are examined.

Analytical results for the maximum load carrying capacity, i.e., the ultimate strength of fixed-end

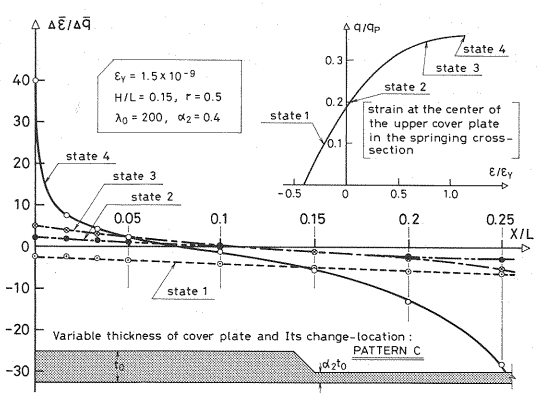

Fig. 5 Incremental Strain Mode at each Loading Step (for variable cross-section of PATTERN-C).

Table 1 Comparison of Analytically Calculated Ultimate Strength with Predicted Strength (for various values of r and α_2).

r	α_2	$\frac{q^*_{max}}{q_p}$	k	$k_{proposal}$	$\frac{(1-k)-(1-k_{prop.})}{(1-k)}$	$\bar{\alpha}$	$\bar{\pi}$	F_c
(1)	(2)	(3)	(4)	(5)	(6)	(7)	(8)	(9)
0	0.4	0.2500	0.2656	0.2294	-4.9 %	0.8395	0.1456	0.970
	0.6	0.2810	0.1745	0.1529	-2.6	0.8584	0.1485	0.994
	0.8	0.3114	0.0852	0.0765	-1.0	0.8726	0.1509	1.010
	1.0	0.3404	0	0	0	0.8809	0.1524	1.020
0.5	0.4	0.3546	0.2268	0.2294	0.3	0.6060	0.3089	0.989
	0.6	0.3919	0.1454	0.1529	0.9	0.6093	0.3106	0.995
	0.8	0.4260	0.0711	0.0765	0.6	0.6075	0.3097	0.992
	1.0	0.4586	0	0	0	0.6040	0.3079	0.986
0.75	0.4	0.4426	0.2215	0.2294	1.0	0.3887	0.4498	0.988
	0.6	0.4890	0.1398	0.1529	1.5	0.3906	0.4521	0.993
	0.8	0.5298	0.0681	0.0765	0.9	0.3882	0.4493	0.987
	1.0	0.5685	0	0	0	0.3847	0.4452	0.978
0.99	0.4	0.6100	0.2385	0.2294	1.2	0.0492	0.7048	1.007
	0.6	0.6810	0.1499	0.1529	0.4	0.0500	0.7158	1.023
	0.8	0.7436	0.0718	0.0765	1.7	0.0501	0.7169	1.036
	1.0	0.8011	0	0	0	0.0498	0.7133	1.019

H/L=0.15, λ_0=200, ε_Y=1.5×10⁻⁹, $\bar{\lambda}$=1.6866

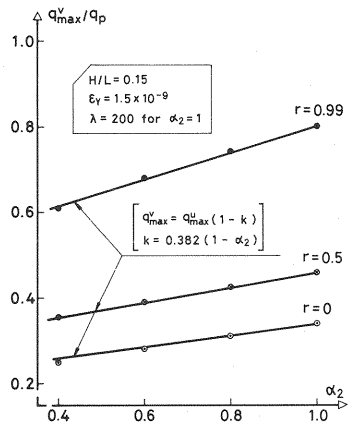

Fig. 6 Relationship between Ultimate Load Intensity and Reduced Thickness Factor (for various values of r).

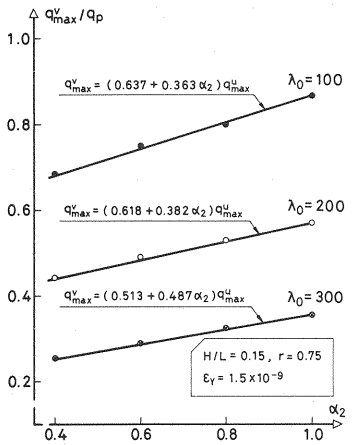

Fig. 7 Relationship between Ultimate Load Intensity and Reduced Thickness Factor (for various values of λ_0)

arches with the variable cross section of Pattern B, q^v_{max}, for various ranges of rise-to-span ratio (H/L= 0.1~0.3), slenderness ratio (λ_0=100~300), yield strain (ε_Y=1.1×10^{-9}~2.3×10^{-9}), load intensity ratio (r=0~0.99), and reduced thickness factor (α_2=0.4~1.0) are compared with the results of the fixed arches with uniform cross-sections ($\alpha_1=\alpha_2=1$), q^u_{max}. The two types of arches have identical magnitude of the slenderness ratio, the rise-to-span ratio, the material properties and the load intensity ratio. Typical results on the strengths, q^v_{max}, are compared with those on, q^u_{max}, in Table 1 for various values of r and α_2, in Table 2 for various values of H/L and α_2 and in Table 3 for various values of $\bar{\lambda}$ and α_2, where $\bar{\lambda}$ is the equivalent slenderness ratio parameter for the equivalent hinged-arch established by the so-called effective length concept[3], as follows;

$$\bar{\lambda}=K\lambda_0\sqrt{\varepsilon_Y}/\pi \quad \cdots\cdots (1.1) \qquad ; K=0.716-0.249\,H/L \quad \cdots\cdots (1.2)$$

Some selected q^v_{max} are plotted in Figs. 6 and 7 by circular marks as a function of α_2 for r-values of 0, 0.5 and 0.99, and for λ_0-values of 100, 200 and 300, in which the ultimate loads of the fixed arches with uniform cross-sections, q^u_{max}, are plotted at α_2=1. From these figures, it can be observed that the ultimate load, q^v_{max}, and the reduced thickness factor, α_2, show well linear relationship for the various values of r or λ_0 or both of them. In Columns of (4) in the Table 1, 2 and 3, the ratio of reduction of the ultimate strength by the effect of variable cross-sectioning, $(q^u_{max}-q^v_{max})$, to the ultimate strength of the arch with uniform cross-section, q^u_{max}, is also tabulated. This ratio, k, can be used to study a proposal for practical estimate of the effect of reduced cross-sectioning on the ultimate strengths of fixed arches.

From these tables, it can be also read that the ratio, k, and the reduced thickness factor, α_2, shows well linear relationship regardless of change of the r-value and for various values of slenderness ratio parameters, $\bar{\lambda}$. Therefore, the k can be formulated practically:

$$q^v_{max}=(1-k)q^u_{max} \quad \cdots\cdots (2.1) \qquad ; k=\varkappa(1-\alpha_2) \quad \cdots\cdots (2.2)$$

By applying a regression analysis to the analytical results for the q^v_{max} and q^u_{max}, the relationship between $\varkappa$ in Eq. (2.2) and the structural parameters are obtained eventually as follows:

$$\varkappa=0.0601\,\bar{\lambda}^2-0.1297\,\bar{\lambda}+0.4301 \quad \cdots\cdots (3)$$

Combining Eqs. (2) and (3) gives

$$k=(0.0601\,\bar{\lambda}^2-0.1297\,\bar{\lambda}+0.4301)(1-\alpha_2) \quad \cdots\cdots (4)$$

This proposed formula is also shown by the solid lines in Figs. 6 and 7 and in the Columns of (5) in the Table 1, 2 and 3. Typical results for the difference between the coefficient factors, $(1-k)$, by the ultimate strength analysis and by the practical formula proposed by Eq. (4) is listed in the Columns of (6) in the Tables 1, 2 and 3. The differences are within the range of −5 % and +3 % for the domain studied in

Table 2 Comparison of Analytically Calculated Ultimate Strength with Predicted Strength (for various values of H/L and α_2).

H/L	α_2	$\frac{q^v_{max}}{q_0}$	k	$k_{proposed}$	$\frac{(1-k)-(1-k_{prop.})}{(1-k)}$	$\bar{m}$	$\bar{n}$	F_c
(1)	(2)	(3)	(4)	(5)	(6)	(7)	(8)	(9)
0.1	0.4	0.4464	0.2303	0.2308	0.0 %	0.3137	0.4806	0.934
	0.6	0.4986	0.1403	0.1538	1.6	0.3185	0.4880	0.948
	0.8	0.5420	0.0655	0.0769	1.2	0.3174	0.4863	0.945
	1.0	0.5800	0	0	0	0.3135	0.4804	0.934
0.15	0.4	0.4426	0.2215	0.2294	1.0	0.3887	0.4498	0.988
	0.6	0.4890	0.1398	0.1529	1.5	0.3906	0.4521	0.993
	0.8	0.5298	0.0681	0.0765	0.9	0.3882	0.4493	0.987
	1.0	0.5685	0	0	0	0.3847	0.4452	0.979
0.3	0.4	0.4746	0.1994	0.2256	3.3	0.4967	0.4004	1.086
	0.6	0.5186	0.1252	0.1504	2.9	0.4947	0.3988	1.082
	0.8	0.5560	0.0621	0.0752	1.4	0.4872	0.3928	1.066
	1.0	0.5928	0	0	0	0.4804	0.3873	1.051

r=0.75, λ_0=200, ε_Y=1.5×10^{-3}

Table 3 Comparison of Analytically Calculated Ultimate Strength with Predicted Strength (for various values of $\bar{\lambda}$ and α_2).

$\bar{\lambda}$	α_2	$\frac{q^v_{max}}{q_0}$	k	$k_{proposed}$	$\frac{(1-k)-(1-k_{prop.})}{(1-k)}$	m	n	F_c
(1)	(2)	(3)	(4)	(5)	(6)	(7)	(8)	(9)
0.8432	0.4	0.6864	0.2088	0.2181	1.2 %	0.3403	0.6866	1.042
	0.6	0.7500	0.1354	0.1454	1.2	0.3402	0.6864	1.042
	0.8	0.8000	0.0778	0.0727	-0.6	0.3344	0.6747	1.024
	1.0	0.8675	0	0	0	0.3362	0.6785	1.030
1.6866	0.4	0.4426	0.2215	0.2294	1.0	0.3887	0.4498	0.988
	0.6	0.4890	0.1398	0.1529	1.5	0.3906	0.4521	0.993
	0.8	0.5298	0.0681	0.0765	0.9	0.3882	0.4493	0.987
	1.0	0.5685	0	0	0	0.3847	0.4452	0.979
2.5300	0.4	0.2560	0.2797	0.2920	1.7	0.3566	0.2827	1.032
	0.6	0.2919	0.1787	0.1947	1.9	0.3574	0.2834	1.034
	0.8	0.3254	0.0844	0.0973	1.4	0.3555	0.2818	1.028
	1.0	0.3554	0	0	0	0.3505	0.2779	1.015

H/L=0.15, r=0.75, ε_Y=1.5×10^{-3}

this paper and their average is 0.5 %. Thus, it may be concluded that the proposed formula gives reasonable correlation.

3. DESIGN CONSIDERATIONS

For the fixed arch with variable cross-section, the calculated strength is q^v_{max}. The load q^v_{max} is applied to a replaced hinged arch (its slenderness ratio=λ_0) which is the same as the fixed arch in all respects except that the supports are hinged and the cross section is uniform over the arch axis ($\alpha_1=\alpha_2=1$). The axial thrust $\overline{N}_0$ and the bending moment $\overline{M}_0$ at the critical quarter point of the replaced arch are determined from a first-order-elastic analysis at the load q^v_{max} as follows:

$$\overline{N}_0=k_n q^v_{max}\ ;\ \overline{M}_0/L=k_m q^v_{max} \quad (5)$$

in which k_n and k_m are constants for a given H/L ratio and r value. Substituting Eq. (2.1) to Eq. (5) gives:

$$\overline{N}_0/(1-k)=k_n q^u_{max}\ ;\ \overline{M}_0/[(1-k)L]=k_m q^u_{max} \quad (6)$$

From Ref. 3), the ultimate load of the fixed arch with uniform cross-section ($\alpha_1=\alpha_2=1$), q^u_{max} is practically equal to that of so-called equivalent hinged arch with effective span length KL, where K is the effective length factor given by Eq. (1.2).

The equivalent arch is analyzed by the convenient first-order-elastic analysis at its ultimate load q^u_{max} and the resulting axial thrust $\hat{N}$ and bending moment $\hat{M}$ at the critical quarter point are:

$$\hat{N}=k_n q^u_{max}\ ;\ \hat{M}/(KL)=k_m q^u_{max} \quad (7)$$

Combining Eqs. (6) and (7) gives:

$$\hat{N}=\overline{N}_0/(1-k)\ ;\ \hat{M}=K\overline{M}_0/(1-k) \quad (8)$$

Thus, an ultimate design formula for the fixed arch with variable cross-section can be obtained by substituting Eq. (8) to the ultimate design criterion for the equivalent hinged arch which is available in Ref. 3) as follows:

$$a\left[\frac{\hat{M}}{M_Y}\right]^2+b\left[\frac{\hat{M}}{M_Y}\right]+c\left[\frac{\hat{N}}{N_Y}\right]\leqq 1 \text{ for } \frac{\hat{N}}{N_Y}>n_{cr} \quad (9.1)$$

$$\alpha\left[\frac{\hat{M}}{M_Y}\right]+\beta\left[\frac{\hat{N}}{N_Y}\right]\leqq 1 \text{ for } \frac{\hat{N}}{N_Y}\leqq n_{cr} \quad (9.2)$$

$$\frac{\hat{M}}{M_Y}=\frac{K\overline{M}_0}{(1-k)N_Y}\ ;\ \frac{\hat{N}}{N_Y}=\frac{\overline{N}_0}{(1-k)N_Y} \quad (9.3)$$

in which N_Y is the squash axial thrust for the springing cross section and M_Y its yield bending moment. The a, b, c, α and β are empirical coefficients and n_{cr} is a nondimensional axial thrust. These coefficients and n_{cr} are depending on the H/L and the equivalent slenderness ratio parameter, $\bar{\lambda}$, given by Eq. (1). Namely:

$a=2.509-1.689\,\bar{\lambda}$; $b=-1.213+1.605\,\bar{\lambda}-0.135\,\bar{\lambda}^2$; $c=(1.824-0.914\,\bar{\lambda}+0.376\,\bar{\lambda}^2)(0.82+1.2\,H/L)$;
$\alpha=1/m_p$; $\beta=(m_p-m_{cr})/(m_p n_{cr})$; $m_p=1.172-0.0469\,\bar{\lambda}$; $n_{cr}=(1-bm_{cr}-am_{cr}^2)/c$;
$m_{cr}=m_p$ for $(am_p^2+bm_p-1)/a\leqq 0$, $m_{cr}=m_p-\sqrt{(am_p^2+bm_p-1)/a}$ for $(am_p^2+bm_p-1)/a>0$.

For demonstration of the accuracy of the limit state design formulas-Eqs. (9.1), (9.2) and (9.3) -proposed herein, comparison with the exact values calculated by the ultimate strength analysis are made for various ranges of the structural parameters mentioned earlier. The accuracy of this formula in predicting the strength of the fixed arches with variable cross-sections is demonstrated in Figs. 8, 9 and 10 for $\alpha_2=0.4$, 0.8 and 1.0, respectively. The solid lines in these figures illustrate the design formula given by Eqs. (9), and circular marks show the analyzed results. Eventually, these results are determined from Eqs. (5) and (8) as follows:

$$\hat{n}=\frac{\hat{N}}{N_Y}=\frac{k_n q_{\max}^v}{(1-k)N_Y};\quad \hat{m}=\frac{\hat{M}}{M_Y}=\frac{KLk_m q_{\max}^v}{(1-k)M_Y} \qquad (10)$$

in which the $q_{\max}^v$ is calculated by the ultimate strength analysis for the fixed-end arch with variable cross-section, and k_n and k_m are analyzed by a first-order-elastic analysis for the replaced hinged arch corresponding to the reference fixed-end arch. It will be seen from these figures that the results predicted by the proposed design formula and analyzed by the ultimate strength analysis agree fairly well. Some typical results for the comparison are also summarized in the Tables 1, 2 and 3, where it is performed using a correlation factor F_c in the Table-Column of (9). The factor is obtained by solving equations as follows:

$$a\left[\frac{\hat{m}}{F_c}\right]^2+b\left[\frac{\hat{m}}{F_c}\right]+c\left[\frac{\hat{n}}{F_c}\right]=1 \text{ for } \frac{\hat{n}}{F_c}>n_{cr} \qquad (11.1)$$

$$a\left[\frac{\hat{m}}{F_c}\right]+\beta\left[\frac{\hat{n}}{F_c}\right]=1 \text{ for } \frac{\hat{n}}{F_c}\leqq n_{cr} \qquad (11.2)$$

in which the $\hat{n}$ and $\hat{m}$ are analytically determined by Eq. (10) and listed in the Table-Columns of (7) and (8). The correlation factors for the thirty-two cases listed in these tables are gathering between 0.934 and 1.051 and their average is 1.009 (0.9 %). Therefore, it may be concluded that the design formulas proposed by Eqs. (9) evaluate the ultimate strengths of the fixed-end steel arch ribs with variable cross-sections accurately enough for practical purpose.

In the design process, $\overline{N}_0$ and $\overline{M}_0$ in Eqs. (9) are axial thrust and bending moment at the critical quarter

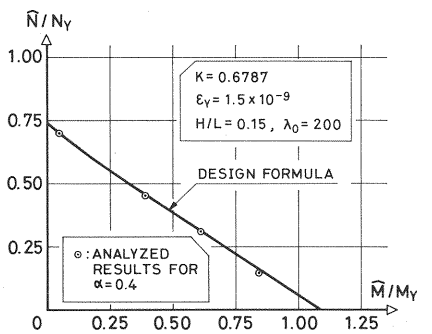

Fig. 8 Comparison of Results Predicted by the Design Formula with those Calculated by the Ultimate Strength Analysis (for $\alpha_2=0.4$).

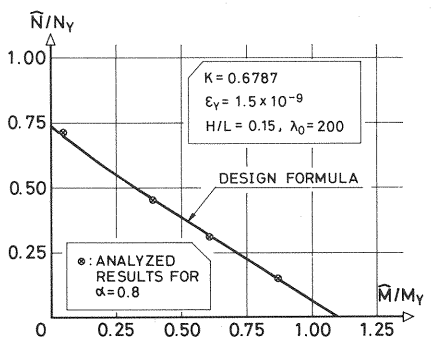

Fig. 9 Comparison of Results Predicted by the Design Formula with those Calculated by the Ultimate Strength Analysis (for $\alpha_2=0.8$).

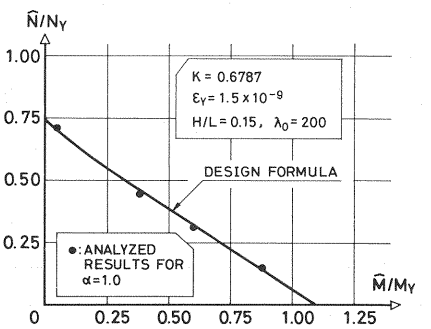

Fig. 10 Comparison of Results Predicted by the Design Formula with those Calculated by the Ultimate Strength Analysis (for $\alpha_2=1.0$).

point of the replaced hinged arch ($\alpha_1=\alpha_2=1$). They are determined by the convenient first-order-elastic analysis for a factored design load of the fixed arch with variable cross-section which is going to be designed. The restrict effect of the fixed-end supports on the ultimate strength is considered by the previously proposed effective length foctor K given by Eq. (1). Moreover, the effect of variable cross-sectioning is evaluated by the factor of k formulated by Eq. (4). Thus, neither first-order-elastic analysis nor instability analysis need to be performed on the fixed arches with variable cross-sections. The loading condition usually involves dead load over the entire span and live load (including impact) over half of the span.

4. CONCLUDING REMARKS

The above conclusions and recommendations are based on the over-all ultimate strengths of the fixed arch ribs with variable cross-sections and on a limited amount of theoretical work within the structural parameter range of the practical steel arch bridge structures. Research is clearly needed on defining the rotation capacity at the springings for the elasto-plastic deformation. Results currently to hand suggest that the evaluation formula of Eq. (4) can be satisfied for most variable cross-sections, which transfer the cross-sectional stresses smoothly over the practical range of reduced magnitude of the plate thickness and its location used in the steel arch bridges. As these simplified criteria are easier to use, it can be recommended for practical designing. Finally, the authors are grateful to Mr. N. Tokashiki of the Department of Civil Engineering at University of Ryukyu for drawings and typings of the manuscript.

REFERENCES

1) Komatsu, S. : Stability and Strength of Braced Steel Arches, Chapter 9 of Steel Framed Structures edited by Narayanan, Elsver Science Publ, London, 1985.
2) Yabuki, T., Vinnakota, S. and Kuranishi, S. : Fixed-End Restraint Effect on Steel Arch Strength, Proc. of ASCE, Journal of Structural Engineering, Vol. 112, No. 4, pp. 653~664, April, 1986.
3) Yabuki, T., Lu, L. W. and Kuranishi, S. : An Ultimate Strength Design Aid For Fixed-End Steel Arches, Proc. of JSCE, Structural Eng. / Earthquake Eng., Vol. 4, No. 1, pp. 740~749, April, 1987.
4) JAPAN LOAD ASSOCIATION, Specification for Highway Bridges, February, 1980 (in Japanese).

(Received April 20 1987)